UC San Diego
UC San Diego Previously Published Works

Title

Depression-like behaviour in mice is associated with disrupted circadian rhythms in nucleus accumbens and periaqueductal grey

Permalink

https://escholarship.org/uc/item/5fq433g5

Journal

European Journal of Neuroscience, 43(10)

ISSN

0953-816X

Authors

Landgraf, Dominic
Long, Jaimie E
Welsh, David K

Publication Date

2016-05-01

DOI

10.1111/ejn.13085

Peer reviewed

Depression-Like Behavior in Mice is Associated with Disrupted Circadian Rhythms in Nucleus Accumbens and Periaqueductal Gray

Dominic Landgraf[1, 2, *], Jaimie E. Long[1, 2] & David K. Welsh[1, 2]

[1]Veterans Affairs San Diego Healthcare System, San Diego, CA

[2]Department of Psychiatry, and Center for Circadian Biology, University of California, San Diego, La Jolla, CA

*Corresponding author: Dominic Landgraf, Department of Psychiatry, University of California, San Diego, 9500 Gilman Drive MC-0603, La Jolla, CA 92093-0603; e-mail:

dlandgraf@ucsd.edu.

Running Title: Absence of Circadian Brain Rhythms in Helpless Mice

Number of pages: 40

Number of figures: 6

Number of tables: 2

Equations: 0

Whole manuscript: 7360 words

Abstract: 230 words

Introduction: 555 words

Abstract

An association between circadian rhythms and mood regulation is well established, and disturbed circadian clocks are believed to contribute to the development of mood disorders, including major depressive disorder (MDD). The circadian system is coordinated by the suprachiasmatic nucleus (SCN), the master pacemaker in the hypothalamus that receives light input from the retina and synchronizes circadian oscillators in other brain regions and peripheral tissues. Lacking the tight neuronal network that couples single-cell oscillators in the SCN, circadian clocks outside the SCN may be less stable and more susceptible to disturbances, e.g. uncontrollable stress. However, non-SCN circadian clocks have not been studied extensively in rodent models of mood disorders. In the present study, we hypothesized that disturbances of local circadian clocks in mood-regulating brain areas are associated with depression-like behavior in mice. Using the learned helplessness procedure, we evoked depression-like behavior in mice bearing the PER2::LUC circadian reporter, and then examined circadian rhythms of PER2 expression in brain slices from these mice using luminometry and bioluminescence imaging. We found that helplessness is associated with absence of circadian rhythms in the nucleus accumbens and the periaqueductal gray, two of the most critical brain regions within the reward circuit. Our study provides evidence that susceptibility of mice to depression-like behavior is associated with disturbed local circadian clocks in a subset of mood-regulating brain areas, but the direction of causality remains to be determined.

Introduction

Circadian clocks have evolved in many species in order to anticipate recurring daily events. In mammals, the circadian system is controlled by the hypothalamic suprachiasmatic nucleus (SCN), which receives light input from the retina and synchronizes downstream oscillators in other brain areas and in peripheral organs. Circadian rhythms control virtually all physiological processes, ensuring alignment among biological functions and synchronization of the organism with the environment. Thus, it is not surprising that a disrupted circadian system leads to disorders including psychiatric conditions like mood disorders (McCarthy & Welsh, 2012; Morris *et al.*, 2012; Kelleher *et al.*, 2014; Landgraf *et al.*, 2014a; Sancar & Brunner, 2014).

Major depressive disorder (MDD) is a disabling neuropsychiatric disorder characterized by episodes of depressed mood. Clinical characteristics of MDD include disruptions of daily rhythmic processes like sleep, appetite, and social interaction. Physiological processes that defy conscious control, like body temperature rhythms and rhythmic hormone release, are also disrupted in depressed patients (Boyce & Barriball, 2010). Together, these observations suggest a dysregulation of the endogenous circadian clock system in depressed humans. In addition, animal models of depression show disturbed circadian rhythms and, conversely, many animals with clock gene mutations exhibit altered mood-related behavior (Landgraf *et al.*, 2014b).

Mood is regulated by a network of discrete brain areas (Russo & Nestler, 2013). However, anatomically, there is not much known about exactly where circadian rhythms contribute to mood regulation. There is little evidence to implicate the SCN in mood regulation, whereas other

rhythmic brain areas have established roles in this regard (McCarthy & Welsh, 2012). Furthermore, the tight oscillator network within the SCN makes it very robust against genetic or environmental disturbances (Liu *et al.*, 2007; Buhr *et al.*, 2010) whereas other brain areas exhibit less stable circadian rhythms that may be more susceptible to subtle mutations or psychological stress. Accordingly, a human postmortem study showed that circadian rhythms in mood-regulating brain regions of depressed patients are weaker than in control subjects (Li *et al.*, 2013). In addition, the diurnal pattern of clock gene rhythms in the basolateral amygdala of anhedonic mice is disrupted (Savalli *et al.*, 2015). However, the determination of rhythms in this study was based on pooling data across subjects. Thus, it stays unclear whether weaker rhythms in depressed subjects were due to lower amplitude rhythms in individual subjects or poor synchronization with the environment, leading to a broad phase distribution across subjects. In addition, a recent study revealed that unpredictable chronic mild stress (UCMS) leads to decreased circadian amplitude in the SCN, but increased circadian rhythm amplitude in the nucleus accumbens (NAc) (Logan *et al.*, 2015).

Because of the relative fragility of circadian clocks in non-SCN brain areas, we hypothesized that depression-like behavior is associated with abnormal circadian rhythms in specific mood-regulating brain areas of individual subjects. To test this hypothesis, we used a learned helplessness (LH) procedure to induce depression-like behavior in mice carrying a PER2::LUC reporter gene, which permits measurement of circadian rhythms of clock gene expression from brain slices *in vitro*. After LH was performed, we categorized mice based on their behavior (helpless vs. resilient), took brain slices from each mouse, and measured circadian rhythms in mood-regulating brain areas. This paradigm allows longitudinal measurements of circadian

rhythms in brain regions of individual subjects, and thus provides accurate detection of potential

rhythm disturbances. Our data reveal that vulnerability to develop depression-like behavior in

mice is associated with absence of circadian rhythms in the NAc and the periaqueductal gray

(PAG).

Material and methods

Animals and study design

All experiments were done in 8-10 week old male mPer2^{Luciferase} (PER2::LUC) mice. In

PER2::LUC knockin mice, the wild type (WT) circadian clock gene *Period2 (Per2)* has been

replaced by homologous recombination with a construct incorporating the firefly luciferase (Luc)

gene in tandem with WT *Per2*, such that a bioluminescent PER2::LUC fusion protein is

expressed under control of all *Per2* regulatory elements (Yoo *et al.*, 2004). In our mice, the

reporter construct also incorporated an SV40 polyadenylation site to enhance expression levels,

and mice were backcrossed to produce a congenic C57BL/6J background (Welsh *et al.*, 2004).

Mice were maintained in LD 12:12 cycles (12 h light, 12 h dark) at all times. Five days before

starting experiments, mice were single-housed with continuous access to water and food. After

five days of acclimation, mice underwent a three day LH procedure, including two days of

training and one day of testing. On the day after testing, brains were collected to prepare explants

for culture. As part of a different study conducted in parallel, in some mice sucrose preference

was tested, and additional behavioral tests (open field test or tail suspension test) were performed

on the day following LH (data shown in (Landgraf *et al.*, 2015)). From this study, we took 23

resilient and 30 helpless mice to look for PER2::LUC rhythms in their brains. Mice that were

exposed to additional tests showed no circadian abnormalities compared to mice that were not

used for additional tests. We attempted to minimize the number of animals used and animal pain

and distress. Mouse studies were conducted in accordance with regulations of the Institutional

Animal Care and Use Committee at University of California, San Diego.

Learned helplessness

The LH procedure has been described elsewhere (Landgraf *et al.*, 2015). Briefly, the protocol consists of two training days and one testing day. On both training days, at *Zeitgeber time* 9 (ZT9, 9 hours after light on), mice were restrained and received 120 electric tail shocks, each lasting 5 sec, randomly timed within a 60 min session. Shock intensity was gradually increased from 0.25 mA to 0.60 mA: every 15 shocks, the current was increased by 0.05 mA. On the testing day, at ZT6, mice were transferred to shuttle boxes (San Diego Instruments, San Diego, CA, USA). Mice received 30 electric shocks to their feet through the grid floor of the shuttle box. During each test shock (0.10 mA, maximum duration 30 sec), the gate remained open, and mice had a chance to escape the shock by crossing a gate to an adjacent compartment. The schedule in trials #1-5 was fixed ratio (FR) 1 (crossing the gate once in order to escape the shock) (Maier *et al.*, 1995). In the remaining trials #6-30, the schedule was changed to FR-2 (crossing the gate twice in order to escape the shock). The number of escape failures and the escape latency were used as criteria for helplessness.

Brain area cultivation and synchronization treatments

One day after LH testing, at ZT8, mice were anesthetized with isoflurane and killed by cervical dislocation. Brains were isolated and kept in half-frozen Hank's Balanced Salt Solution (HBSS). 300 μm brain slices were prepared with a vibratome (Leica, Buffalo Grove, IL, USA), and specific brain areas were cut out. Tissues were immediately transferred to tissue culture inserts (EMD Millipore, Billerica, MA, USA) and cultured in 35-mm petri dishes containing 1 ml of culture medium [high glucose DMEM (Mediatech, Manassas, VA, USA), 4 mM sodium carbonate, 10 mM HEPES, 52 U/ml penicillin, 52 μg/ml streptomycin, 4 mM L-glutamine, 2%

B-27 (GIBCO, Grand Island, NY, USA), 0.1 mM luciferin (BioSynth, Itasca, IL, USA)]. Unless stated otherwise, tissues were treated with 10 μM forskolin for the first 2 h of culturing in order to enhance rhythmicity.

PER2::LUC measurements in LumiCycle luminometer

Luminescence measurements were done at 10 min intervals using a LumiCycle luminometer (Actimetrics) that was placed inside a 37°C incubator without CO_2. Period, peak phases, and amplitude were determined over 7 days by fitting a sine wave (Sin fit (Damped) for period, phase, and damping time (time to reach 1/e of initial amplitude), LM fit (Sin) for amplitude) to 24 h running average baseline-subtracted data using LumiCycle Analysis software (Actimetrics, Wilmette, IL, USA). The first day of measurement was excluded from analyses. Amplitude was normalized to the total brightness in order to account for different sizes of brain tissue and technical differences between slices. Explants failing to show significant χ^2 periodogram values near 24 h (Sokolove & Bushell, 1978) or a minimum of two PER2::LUC peaks were determined to be arrhythmic.

PER2::LUC bioluminescence imaging

Region-specific and single-cell PER2::LUC measurements were carried out as described elsewhere (Welsh & Noguchi, 2012; Noguchi *et al.*, 2013). Briefly, the culture was placed on the stage of an inverted microscope (Olympus, Tokyo, Japan) in a dark room. A heated lucite chamber (Solent Scientific, Segensworth, UK), kept the samples at a constant 36°C. Light from the sample was collected by an Olympus 4x XLFLUOR objective (NA 0.28) and transmitted directly to a cooled charge-coupled-device (CCD) camera (Spectral Instruments, Tucson, AZ, USA) mounted on the bottom part of the microscope. The camera contained a back-thinned CCD

thermoelectrically cooled to –90 °C with a rated quantum efficiency of 92% at 560 nm. The signal-to-noise ratio was increased by 4 × 4 binning of the 1056 × 1032 pixel array. Images were collected at intervals of 30 min, with 29.5-min exposure duration, for 4-7 days. Images were acquired and saved to a computer with SI Image SGL D software (Spectral Instruments), and analyzed with MetaMorph (Molecular Devices, Sunnyvale, CA, USA).

Data analysis

Statistical analysis was carried out with GraphPad Prism (GraphPad Software, La Jolla, CA, USA), SPSS 20 (IBM, Armok, NY, USA), and Oriana (KCS, Pentraeth, UK). Statistical tests for each study are indicated in the figure legends and supplementary tables S1-S8. Samples with an n<3 were excluded from statistical analyses. Data were checked for normal distribution and homogeneity of variance. For normally distributed data parametric test were used (one-way ANOVA or Student's t-test). If the data were not normally distributed, a nonparametric test was used (Mann-Whitney). For data that were not homogeneously distributed, Welch test was used instead of one-way ANOVA.

Results

Most mood-regulating brain areas are capable of expressing circadian rhythms

In order to assess circadian clock function in mood-regulating brain areas, we measured

PER2::LUC activity of 9 brain structures with reported mood regulation functions, as well as the

SCN. Cultured mood-regulating brain areas were: cingulate cortex area 1 (Cg1), NAc, amygdala

(Amy), lateral habenula (LHb), hippocampus (HIP), PAG, posterior hypothalamic area (PHA),

ventral tegmental area (VTA), the dorsal raphé nucleus (DR). To determine reliability of

rhythmicity, we calculated the percentage of cultured explants (one per region, per mouse) that

were rhythmic. As a measure of rhythm stability we measured the amplitude and the damping

time of PER2::LUC rhythms. In addition, we determined the phasing of the individual regions,

which presumably reflect the phase relationship between mood-regulating brain areas in the

brain. In order to determine baseline rhythms of the brain explants, we first cultured the explants

without any synchronization treatment. In a second experiment, to examine their capability to

express circadian rhythms after synchronizing individual cells, we treated the brain explants with

10 μM forskolin for 2 h prior to recording.

Baseline rhythm measurements

When cultured without synchronization, most mood-regulating brain areas showed unreliable

and weak circadian PER2::LUC rhythms, and some structures were completely arrhythmic (Fig.

1, Table 1). All SCN cultures, on the other hand, showed sustained circadian rhythms. Some

Cg1, PAG, LHb, and VTA cultures showed significant circadian rhythms. NAc, Amy, HIP, PHA

and DR failed to show circadian rhythms. Results for brain area explants cultured without

forskolin synchronization treatment are summarized in Table 1.

Rhythms measurements after synchronization

Forskolin has been shown to synchronize individual cells with each other and induce clock gene

expression to enhance rhythmicity (Yagita & Okamura, 2000). When treated with 10 μM

forskolin for 2 h prior to recording, several previously arrhythmic or weakly rhythmic brain areas

expressed sustained circadian rhythms, and amplitudes were generally higher compared to

cultures without forskolin (Fig. 1, Table 2). Forskolin increased the percentage of rhythmic HIP,

PAG, and PHA cultures. Although most HIP explants showed significant rhythms, the amplitude

of the rhythms was relatively low. Cg1, NAc, LHb, VTA, and DR explants responded only

modestly to forskolin treatment and few cultures became rhythmic. However, compared to Cg1,

LHb, and VTA explants, the amplitude of rhythmic NAc and DR explants was relatively high.

Amy failed to show significant circadian rhythms under the influence of forskolin. Only SCN

explants were unaffected by the forskolin treatment, with all SCN cultures showing robust

circadian rhythms with or without forskolin. Since only a few LHb slices were rhythmic in our

approach, and previous studies reported more pronounced rhythms in this region (Guilding *et al.*,

2010), we investigated LHb PER2::LUC expression with more detailed microscopic imaging

(see supporting information and Fig. S1). Results for brain area explants treated with 10 μM

forskolin are summarized in Table 2.

Helpless mice have normal period, amplitude, <u>but misaligned phase</u> of rhythms in mood-regulating brain areas

To investigate circadian rhythms of mood-regulating brain regions in mice that show depression-

like behavior, we exposed PER2::LUC mice to our LH protocol (Landgraf *et al.*, 2015) and

measured brain area oscillations one day later. We compared rhythms of resilient and helpless mice with rhythms of naive home cage controls. In order to achieve reliable rhythm analyses, we investigated only the circadian oscillations of SCN, NAc, PAG, PHA, and DR explants, because these regions showed robust rhythms in our preliminary screen. Since in our screen, SCN explants showed no differences in response to forskolin synchronization, we only synchronized NAc, PAG, PHA, and DR explants prior to PER2::LUC measurements.

Helplessness had no significant impact on period and amplitude of oscillations in the SCN, or in any of the mood-regulating brain areas investigated (Figs. 2, 3, Tables S1, S2). There were non-significant trends, with period tending to be shorter in the NAc of LH resilient mice than of home cage-control and helpless mice (Fig. 2). When comparing all mice that underwent the LH procedure (whether they became helpless or not) with naive home cage controls, the period of the SCN clock was 0.57 h longer (student's t-test: t_{42}=2.656, p=0.0111) and the amplitude tended to be higher (student's t-test: t_{42}=1.963, p=0.0563) (Fig. 2, 3). Thus, independent of the mood state of the mice, the exposure to stress during LH seems to affect the central circadian clock in the SCN. Compared to resilient mice, the PHA phase of helpless mice was significantly advanced, but phases of all other brain areas were not affected by LH (Fig. 4, Table S3).

Helplessness is associated with absence of circadian rhythms in the NAc and the PAG

While brain slices from helpless mice exhibited no changes in rhythm parameters when rhythms were present, there were differences in the proportion of brain slices exhibiting rhythmicity. About half (54%) of NAc explants from naive home cage controls showed significant circadian

rhythms (Fig. 5, Table S4). But remarkably, after mice underwent the LH procedure, a large

majority of NAc explants from resilient mice showed rhythmic oscillations (81.25%), whereas

significantly fewer NAc explants from helpless mice (33.3%) were rhythmic. PAG explants

showed a similar pattern (Fig. 5, Table S4): whereas not all PAG explants of naive home cage

controls were rhythmic (76.9%), 100% of the PAG explants of resilient mice showed significant

rhythms; and among mice that were helpless after LH, the number of rhythmic PAG cultures was

significantly lower (64.3%). The SCN and PHA both expressed circadian rhythms regardless of

behavioral classification (Fig. 5, Table S4). Thus, there is an association between helplessness

and the absence of circadian rhythms in the brain that is region-specific.

Stress activates circadian rhythms in the dorsal raphé nucleus

The LH procedure activated circadian rhythms in the DR regardless of behavioral outcome after

LH (Fig. 5, Table S4). Only 2 of 10 DR slices of naive home cage controls exhibited detectable

rhythms, but almost all DR explants from mice that underwent the LH procedure were rhythmic.

This effect was not associated with the behavioral outcome as there were no significant

differences between the number of rhythmic slices of resilient (80%) and helpless mice (95%).

Expression of rhythms is regulated differently in different brain areas

Absence of detectable rhythms in a brain explant could be due to lowered amplitudes of single

cell oscillators or desynchronization among the individual single cell oscillators. Since many

NAc and PAG explants are arrhythmic in helpless mice, we sought to determine the nature of

single-cell rhythmicity in NAc and PAG explants. Therefore, we transferred rhythmic and

arrhythmic cultures to a microscope for luminescence imaging of single cells. We confirmed that

NAc and PAG slices that were arrhythmic in the luminometer also showed very faint or no

overall rhythms on the microscope (Fig. S2). Interestingly, forskolin was not able to restore

rhythms in arrhythmic explants. To test whether arrhythmic slices are insensitive to

synchronization treatments, we also imaged luminesces of single cells from arrhythmic NAc and

PAG explants that were not treated with forskolin. We found that the nature of arrhythmicity is

similar in explants from helpless and resilient mice. Hence, we decided to group data based on

their rhythmicity independent of their behavioral phenotype.

Compared to rhythmic NAc cultures, arrhythmic NAc explants contained fewer cells that express

PER2::LUC, resulting in a reduced overall brightness of the slices (Figs. 6A, B, Table S5).

However, although the total PER2::LUC output of arrhythmic NAc slices is lower and not

oscillating, these slices do contain rhythmic individual cells. Forskolin lengthened the period and

increased the amplitude of single cells in arrhythmic and rhythmic brain cultures (Fig. 6C, Table

S5). However, single cell amplitudes of arrhythmic explants were significantly lower. In

addition, the phase distribution of these cells is much broader than for cells in rhythmic NAc

slices (Fig. 6D, Table S6), and the period distribution is also slightly broader (Fig. 6E). In

contrast, rhythmic and arrhythmic PAG slices have similar numbers of PER2::LUC expressing

cells, which is reflected in the similar total brightness of both groups (Fig. 7A, B, Table S7).

Period and amplitude of individual rhythmic cells was also similar in rhythmic and arrhythmic

PAG cultures (Fig. 7C, Table S7). In addition, phase distributions of single cells were much

broader in arrhythmic PAG slices than in rhythmic PAG explants (Fig. 7D, Table S8).

Interestingly, many cells of arrhythmic PAG explants that were treated with forskolin had

unequal periods whereas the majority of individual cells from rhythmic PAG explants and untreated arrhythmic PAG explants displayed similar periods (Fig. 7E).

Together, these results show that although the total output of some NAc and PAG slices is arrhythmic, they still contain cells exhibiting circadian rhythms. In addition, whereas the arrhythmicity of NAc slices arises from both reduced PER2::LUC expression and dephased single-cell rhythms, the arrhythmicity of PAG slices arises primarily from dephasing.

Discussion

In this study we investigated whether depression-like behavior is associated with disturbed circadian rhythms in mood-regulating brain areas. Because these brain areas lack the SCN's neuronal network mediating coupling of single-cell oscillators (Liu *et al.*, 2007), we hypothesized that genetic or environmental disturbances will have a strong impact on circadian clocks in these brain areas, and thereby increase the risk of mood disorders. As a model of depression we chose LH, as helplessness is an important aspect of depression in humans, and mice allow access to brain tissue and use of sophisticated genetic tools, such as circadian reporter genes. Our mouse LH protocol excludes fear conditioning as a possible reason for freezing behavior during testing and provides a valid model of depression-like behavior (Maier & Watkins, 2005; Landgraf *et al.*, 2015). Investigating circadian clock characteristics of four different mood-regulating brain areas and of the SCN, we found that helplessness is associated with the absence of *in vitro* circadian rhythms in the NAc and the PAG. Importantly, in depressed patients, the NAc was one of the brain regions that showed disturbed circadian rhythms in a human postmortem study (Li *et al.*, 2013). However, due to the limitations of studying only one time point per human brain, in that study it could not be determined to what extent dephasing among individual subjects or among cells within a single subject may have contributed to weaker circadian rhythms observed at the population level. In contrast, our approach allowed continuous observation of circadian oscillations of brain regions from mice with depression-like behavior over the course of several days *in vitro*. Thus, we could show that helplessness is <u>associated with arrhythmicity</u> in the NAc and the PAG of individual mice *in vitro*.

In addition, our results suggest that the cellular basis of arrhythmicity differs between the two

brain regions.

Remarkably, when brain areas were rhythmic in our study, period and amplitude did not differ

significantly across groups, i.e. rhythms of NAc and PAG seemed to be either completely absent

or completely normal. Most mice that were resilient to the LH procedure showed circadian

oscillations in NAc and PAG, whereas many mice that were susceptible to LH lacked rhythms in

these two brain regions. Interestingly, compared to explants from home cage control mice, NAc

and PAG cultures from helpless mice were less frequently rhythmic, but cultures from non-

helpless mice were actually more frequently rhythmic. A possible explanation for this result is

that the LH procedure affects rhythms in the NAc and PAG in such a way that, dependent on

whether the mouse becomes helpless or not, rhythms are suppressed or activated. An alternative

explanation, however, is that at baseline the NAc and PAG are rhythmic in some mice and

arrhythmic in others, and that arrhythmicity in these brain regions confers susceptibility to

helplessness when exposed to the LH procedure, whereas rhythmicity confers resilience.

Conceivably, LH sorts the mice into previously existing susceptible and resilient subpopulations

that are at least partly dependent on their ability to express rhythms in the NAc or the PAG.

Interestingly, social defeat stress has previously been associated with lower levels of *Per1* and

Per2 expression in the NAc, and knockdown of *Per1* and *Per2* in the NAc increased anxiety-like

behavior in mice (Spencer *et al.*, 2013), results that are broadly consistent with our present

finding that helpless behavior is associated with absence of circadian rhythms in NAc. However,

and in contrast to our present results, the same group recently reported that UCMS increased

rhythm amplitude in the NAc (Logan *et al.*, 2015). Additionally, UCMS lowered rhythm amplitude in the SCN (Jiang *et al.*, 2011; Logan *et al.*, 2015), whereas SCN amplitude tended to increase after LH in our study. Stress-related changes in brain rhythms may depend on the time of day when the animals were stressed. In our study, using LH, animals were only stressed during their sleep phase (day), whereas UCMS usually also involves stress during the activity phase (night). Alternatively, different approaches to induce depression-like behavior in mice may lead to different circadian rhythm outcomes in NAc and SCN, due to differing types or durations of behavioral manipulation. Since LH requires only three days to induce helpless behavior, we believe that our observations reflect a reduced pre-existing capacity to express NAc and PAG circadian rhythms in mice that are more susceptible to developing helpless behavior. In contrast, exposure to four weeks of UCMS is evidently sufficient to alter rhythms in the NAc (Logan *et al.*, 2015). Interestingly, although our helpless mice are less likely to show NAc rhythms, when rhythms do occur they tend to be of higher amplitude than in non-helpless mice, possibly reflecting the beginnings of a more long-term compensatory response that is more fully developed after four weeks of UCMS.

Compared to resilient mice, PHA rhythms of helpless mice were advanced by ~2.5 hours, leading to a circadian misalignment between the PHA and other brain areas. Conceivably, this may contribute to the development of helpless behavior in mice. Phases of brain area explants were potentially shifted by forskolin. However, the direction and magnitude of phase shifts caused by forskolin depend on the time of administration (Eskin & Takahashi, 1983). We found remarkable phase differences between brain regions (see also Table 2) and significant phase

differences in the PHA of helpless mice. Thus, the phase response to forskolin depends on the prior *in vivo* phase and therefore may be indicative of *in vivo* phase differences between groups.

DR rhythms are activated by the LH procedure, but this effect is independent of whether helpless behavior is induced or not. Possibly, the clock of the DR is very sensitive to stress, but is not directly involved in the development of helplessness. Also, in the SCN, rhythm period is longer and amplitude slightly increased in animals that underwent the LH procedure, but since all LH mice were affected equally regardless of helpless behavior, those changes are likely associated with generalized stress rather than specifically with a helpless behavioral state.

Importantly, differences of circadian rhythms between resilient and helpless mice were region-specific. The regions we studied were previously shown to be involved in LH. C-fos activity in serotonergic cells in the DR is directly activated by stress, especially by inescapable stress as produced by LH (Grahn *et al.*, 1999), and circadian rhythms in a variety of tissues are reset by glucocorticoids (Balsalobre *et al.*, 2000). Thus, stress-related glucocorticoids may activate both DR neuronal activity and the DR circadian clock in parallel. Inescapable stress increases the activity of serotonergic DR neurons projecting to the anterior PAG, which promotes helpless behavior (Schutz *et al.*, 1985; Maier *et al.*, 1993; Maier & Watkins, 2005). Sustained NAc CREB activation also promotes helpless behavior, whereas antagonizing CREB has the opposite effect (Russo & Nestler, 2013). On the other hand, stress also induces ΔFosB in PAG, thereby inhibiting substance P release in the NAc, which in turn reduces helpless behavior (Berton *et al.*, 2007). High substance P levels are associated with depression in humans, and substance P

antagonists are promising candidates as antidepressants (Herpfer & Lieb, 2005). Thus, the

balance of inputs to and signaling within NAc neurons appears to determine susceptibility to LH.

Precisely how the circadian clock might modulate this neuronal circuit determining susceptibility

to LH is not known. Our data show that helpless animals tend to lack rhythms in the NAc and/or

PAG. Conceivably, some component of signaling within this circuit may be altered when these

brain areas are arrhythmic. For example, the circadian clock protein CRY cyclically inhibits

CREB, whose sustained activation in NAc increases vulnerability to LH. Perhaps weakened

circadian clocks in NAc could increase vulnerability to LH via low CRY levels, and consequent

failure of CRY to inhibit CREB signaling at dawn. This could be tested by manipulating CRY or

CREB function in mouse NAc, followed by testing for susceptibility to LH. The insensitivity of

arrhythmic NAc explants to CREB-mediated phase synchronization and amplitude increase by

forskolin (Fig. 6C, D, E) may support the idea of elevated CREB levels in the NAc of helpless

mice. Elevated CREB levels may limit the dynamic range of synchronization and amplitude in

response to forskolin.

A connection between disturbed circadian clocks and depression is indisputable, but it is not

clear whether disturbed circadian clocks lead to MDD or whether they are rather a symptom of

MDD (Landgraf et al., 2014b). In the present study, we demonstrate that helplessness, which is a

central aspect of MDD, is associated with absence of in vitro circadian rhythms in the NAc and

the PAG, which are both directly involved in the development of helpless behavior. However, it

is still unknown whether the lack of rhythms in NAc and PAG explants is a consequence of the

LH procedure, or whether a pre-existing lack of rhythmicity increases susceptibility to helpless

behavior. Examining behavior of animals after region-specific manipulations of the circadian

clock in mood-regulating brain areas may help to determine whether a disturbed clock in these

structures causes depression-like behavior. In addition, the role of local brain circadian rhythms

in the regulation of sensitivity to stress remains unclear. Studying the consequences of

experimentally disrupted local circadian clocks may reveal whether and how circadian clock

disturbances alter physiological responses to stress.

Acknowledgment:

Abbreviations

Amy, amygdala; Cg1, cingulate cortex area 1; DR, dorsal raphé nucleus; HIP, hippocampus; LH, learned helplessness; LHb, lateral habenula; MDD, major depressive disorder; NAc, nucleus accumbens; PAG, periaqueductal gray; PER2::LUC, PERIOD2::LUCIFERASE; PHA, posterior hypothalamic area; SCN, suprachiasmatic nucleus; UMCS, unpredictable chronic mild stress; VTA, ventral tegmental area; WT, wild type; ZT, Zeitgeber

References

Balsalobre, A., Brown, S.A., Marcacci, L., Tronche, F., Kellendonk, C., Reichardt, H.M., Schutz, G. & Schibler, U. (2000) Resetting of circadian time in peripheral tissues by glucocorticoid signaling. *Science*, **289**, 2344-2347.

Berton, O., Covington, H.E., 3rd, Ebner, K., Tsankova, N.M., Carle, T.L., Ulery, P., Bhonsle, A., Barrot, M., Krishnan, V., Singewald, G.M., Singewald, N., Birnbaum, S., Neve, R.L. & Nestler, E.J. (2007) Induction of deltaFosB in the periaqueductal gray by stress promotes active coping responses. *Neuron*, **55**, 289-300.

Boyce, P. & Barriball, E. (2010) Circadian rhythms and depression. *Australian family physician*, **39**, 307-310.

Buhr, E.D., Yoo, S.H. & Takahashi, J.S. (2010) Temperature as a universal resetting cue for mammalian circadian oscillators. *Science*, **330**, 379-385.

Grahn, R.E., Will, M.J., Hammack, S.E., Maswood, S., McQueen, M.B., Watkins, L.R. & Maier, S.F. (1999) Activation of serotonin-immunoreactive cells in the dorsal raphe nucleus in rats exposed to an uncontrollable stressor. *Brain research*, **826**, 35-43.

Guilding, C., Hughes, A.T. & Piggins, H.D. (2010) Circadian oscillators in the epithalamus. *Neuroscience*, **169**, 1630-1639.

Herpfer, I. & Lieb, K. (2005) Substance P receptor antagonists in psychiatry: rationale for development and therapeutic potential. *CNS drugs*, **19**, 275-293.

Jiang, W.G., Li, S.X., Zhou, S.J., Sun, Y., Shi, J. & Lu, L. (2011) Chronic unpredictable stress induces a reversible change of PER2 rhythm in the suprachiasmatic nucleus. *Brain research*, **1399**, 25-32.

Kelleher, F.C., Rao, A. & Maguire, A. (2014) Circadian molecular clocks and cancer. *Cancer letters*, **342**, 9-18.

Landgraf, D., Long, J., Der-Avakian, A., Streets, M. & Welsh, D.K. (2015) Dissociation of learned helplessness and fear conditioning in mice: a mouse model of depression. *PloS one*, **10**, e0125892.

Landgraf, D., McCarthy, M.J. & Welsh, D.K. (2014a) Circadian clock and stress interactions in the molecular biology of psychiatric disorders. *Current psychiatry reports*, **16**, 483.

Landgraf, D., McCarthy, M.J. & Welsh, D.K. (2014b) The role of the circadian clock in animal models of mood disorders. *Behavioral neuroscience*, **128**, 344-359.

Li, J.Z., Bunney, B.G., Meng, F., Hagenauer, M.H., Walsh, D.M., Vawter, M.P., Evans, S.J., Choudary, P.V., Cartagena, P., Barchas, J.D., Schatzberg, A.F., Jones, E.G., Myers,

R.M., Watson, S.J., Jr., Akil, H. & Bunney, W.E. (2013) Circadian patterns of gene expression in the human brain and disruption in major depressive disorder. *Proceedings of the National Academy of Sciences of the United States of America*, **110**, 9950-9955.

Liu, A.C., Welsh, D.K., Ko, C.H., Tran, H.G., Zhang, E.E., Priest, A.A., Buhr, E.D., Singer, O., Meeker, K., Verma, I.M., Doyle, F.J., 3rd, Takahashi, J.S. & Kay, S.A. (2007) Intercellular coupling confers robustness against mutations in the SCN circadian clock network. *Cell*, **129**, 605-616.

Logan, R.W., Edgar, N., Gillman, A.G., Hoffman, D., Zhu, X. & McClung, C.A. (2015) Chronic Stress Induces Brain Region-Specific Alterations of Molecular Rhythms that Correlate with Depression-like Behavior in Mice. *Biological psychiatry*.

Maier, S.F., Grahn, R.E., Kalman, B.A., Sutton, L.C., Wiertelak, E.P. & Watkins, L.R. (1993) The role of the amygdala and dorsal raphe nucleus in mediating the behavioral consequences of inescapable shock. *Behavioral neuroscience*, **107**, 377-388.

Maier, S.F., Grahn, R.E. & Watkins, L.R. (1995) 8-OH-DPAT microinjected in the region of the dorsal raphe nucleus blocks and reverses the enhancement of fear conditioning and interference with escape produced by exposure to inescapable shock. *Behavioral neuroscience*, **109**, 404-412.

Maier, S.F. & Watkins, L.R. (2005) Stressor controllability and learned helplessness: the roles of the dorsal raphe nucleus, serotonin, and corticotropin-releasing factor. *Neuroscience and biobehavioral reviews*, **29**, 829-841.

McCarthy, M.J. & Welsh, D.K. (2012) Cellular circadian clocks in mood disorders. *Journal of biological rhythms*, **27**, 339-352.

Morris, C.J., Yang, J.N. & Scheer, F.A. (2012) The impact of the circadian timing system on cardiovascular and metabolic function. *Progress in brain research*, **199**, 337-358.

Noguchi, T., Wang, L.L. & Welsh, D.K. (2013) Fibroblast PER2 circadian rhythmicity depends on cell density. *Journal of biological rhythms*, **28**, 183-192.

Russo, S.J. & Nestler, E.J. (2013) The brain reward circuitry in mood disorders. *Nature reviews. Neuroscience*, **14**, 609-625.

Sancar, G. & Brunner, M. (2014) Circadian clocks and energy metabolism. *Cellular and molecular life sciences : CMLS*, **71**, 2667-2680.

Schutz, M.T., de Aguiar, J.C. & Graeff, F.G. (1985) Anti-aversive role of serotonin in the dorsal periaqueductal grey matter. *Psychopharmacology*, **85**, 340-345.

Sokolove, P.G. & Bushell, W.N. (1978) The chi square periodogram: its utility for analysis of circadian rhythms. *Journal of theoretical biology*, **72**, 131-160.

Spencer, S., Falcon, E., Kumar, J., Krishnan, V., Mukherjee, S., Birnbaum, S.G. & McClung, C.A. (2013) Circadian genes Period 1 and Period 2 in the nucleus accumbens regulate anxiety-related behavior. *The European journal of neuroscience*, **37**, 242-250.

Welsh, D.K. & Noguchi, T. (2012) Cellular bioluminescence imaging. *Cold Spring Harbor protocols*, **2012**.

Welsh, D.K., Yoo, S.H., Liu, A.C., Takahashi, J.S. & Kay, S.A. (2004) Bioluminescence imaging of individual fibroblasts reveals persistent, independently phased circadian rhythms of clock gene expression. *Current biology : CB*, **14**, 2289-2295.

Yagita, K. & Okamura, H. (2000) Forskolin induces circadian gene expression of rPer1, rPer2 and dbp in mammalian rat-1 fibroblasts. *FEBS letters*, **465**, 79-82.

Yoo, S.H., Yamazaki, S., Lowrey, P.L., Shimomura, K., Ko, C.H., Buhr, E.D., Siepka, S.M., Hong, H.K., Oh, W.J., Yoo, O.J., Menaker, M. & Takahashi, J.S. (2004) PERIOD2::LUCIFERASE real-time reporting of circadian dynamics reveals persistent circadian oscillations in mouse peripheral tissues. *Proceedings of the National Academy of Sciences of the United States of America*, **101**, 5339-5346.

Tables

Table 1: Summary of SCN and mood-regulating brain area PER2::LUC rhythms *in vitro* without any special synchronization treatment. Cultures that showed at least two PER2::LUC rhythm peaks and significant rhythmicity in periodogram analysis were defined as rhythmic. For analysis of rhythm parameters, 4-5 days of PER2::LUC data excluding the first day of measurement were used. Damping time is the number of days required for the amplitude of the rhythm to decrease to $1/e$ ($\approx$36.8 %) of the starting value. Phase is given as the time of day of the second PER2::LUC peak relative to the animal's previous LD cycle, with light onset = ZT0. Values of damping time and phase are given as mean $\pm$ SEM; numbers of explants (n) are indicated in parentheses.

| Brain area | **Without synchronization** | | | | |
	% rhythmic (n)	Period (h)	Normalized amplitude	Damping time (days)	Phase (ZT)
SCN	100 (30)	24.9 ± 0.2	0.129 ± 0.012	5.0 ± 0.7	15.6 ± 0.9
Cg1	14 (7)	23.8	0.015	5.3	22.3
NAc	0 (6)	---	---	**---**	---
Amy	0 (3)	---	---	---	---
LHb	38 (13)	23.3 ± 1.6	0.029 ± 0.004	4.7 ± 0.3	13.5 ± 1.8
HIP	0 (11)	---	---	---	---
PAG	44 (9)	25.7 ± 0.6	0.03 ± 0.004	9.0 ± 5.7	19.4 ± 1.4
PHA	0 (4)	---	---	---	---
VTA	31 (13)	26.3 ± 0.5	0.024 ± 0.005	3.3 ± 0.3	0.5 ± 0.5
DR	0 (2)	---	---	---	---

Table 2: Summary of SCN and mood-regulating brain area PER2::LUC rhythms *in vitro* after synchronization with 10 µM forskolin. Indications as in Table 1.

Brain area	% rhythmic (n)	Period (h)	Normalized amplitude	Damping time (days)	Phase (ZT)
With synchronization					
SCN	100 (10)	24.1 ± 0.4	0.108 ± 0.014	2.9 ± 0.2	15.9 ± 0.4
Cg1	33 (6)	23.4 ± 0.8	0.018 ± 0.007	6.1	1.3 ± 3.1
NAc	54 (13)	28.1 ± 1.8	0.053 ± 0.005	2.3 ± 0.7	16.5 ± 1.5
Amy	0 (4)	---	---	---	---
LHb	0 (4)	---	---	---	---
HIP	80 (5)	25.9 ± 0.3	0.011 ± 0.0003	14.9 ± 2.3	21.1 ± 0.3
PAG	77 (13)	24.7 ± 0.5	0.031 ± 0.004	4.7 ± 1.0	4.8 ± 0.9
PHA	80 (11)	25.0 ± 0.4	0.033 ± 0.004	6.6 ± 2.3	21.7 ± 1.6
VTA	0 (5)	---	---	---	---
DR	20 (10)	25.0 ± 3.2	0.026 ± 0.006	7.4 ± 0.6	17.9 ± 6.7

Figure legends

Fig. 1: Some mood-regulating brain areas are capable of expressing circadian rhythms *in vitro*.

Left panel: Without any special treatment to synchronize cellular oscillators within brain slices,

most mood-regulating brain areas show no circadian PER2::LUC rhythms. Only some Cg1,

LHb, PAG, and VTA explants showed relatively strong circadian rhythms with more than 2

peaks under such conditions. Right panel: When cultured brain slices were treated with 10 uM

forskolin to synchronize cellular oscillators before PER2::LUC measurement started, SCN, PAG,

NAc, PHA, and DR expressed prominent circadian rhythms with at least four PER2::LUC

expression peaks, and HIP and Cg1 expressed weaker rhythms, whereas Amy, LHb, and VTA

explants failed to show sustained rhythms.

Fig. 2: The extent of helplessness is not associated with abnormal circadian periods in mood-

regulating brain areas. The circadian period in the SCN and different mood-regulating brain

areas is similar in resilient and helpless mice. The corresponding brain areas of naive home cage-

control mice show similar circadian periods. Data are shown as mean ± SEM; (1-way ANOVA

with Bonferroni post test comparing all groups with each other); n-values are shown in brackets.

Fig. 3: When circadian PER2::LUC rhythms are present in brain slices, the extent of helplessness

is not associated with abnormal amplitudes. The amplitude of PER2::LUC rhythms in the SCN

and different mood-regulating brain areas is similar in resilient and helpless mice. The

corresponding brain areas of naive home cage-control mice show similar circadian amplitudes.

Data are shown as mean ± SEM; (1-way ANOVA with Bonferroni post test comparing all groups with each other); n-values as indicated in Fig. 2.

Fig. 4: When circadian PER2::LUC rhythms are present in brain slices, the extent of helplessness is not associated with abnormal phases. Compared to resilient mice, the PHA phase of helpless mice is advanced. The phase of PER2::LUC rhythms in the SCN and the other mood-regulating brain areas is similar in resilient and helpless mice. The corresponding brain areas of naive home cage-control mice show similar circadian phases. Data are shown as mean ± SEM; *$p \leq 0.05$ (1-way ANOVA with Bonferroni post test comparing all groups with each other); n-values as indicated in Fig. 2.

Fig. 5: The extent of helplessness is associated with absence of circadian PER2::LUC rhythms in a subset of mood-regulating brain areas. Significantly fewer cultured NAc and PAG slices were rhythmic for helpless mice than for resilient mice. Cultured NAc slices of naive home cage control mice are also less frequently rhythmic than cultured NAc slices of resilient mice that underwent the LH procedure. Compared to home cage controls, DR slices from mice exposed to the LH procedure are more frequently rhythmic, regardless of whether the mice become helpless. Rhythmicity of the SCN and the PHA is not affected by LH. Data are shown as percentage of slices that are significantly rhythmic; *$p \leq 0.05$, **$p \leq 0.01$, ***$p \leq 0.001$ (Fisher's exact test); n=10-16.

Fig. 6: Single-cell characterization of rhythmic and arrhythmic NAc organotypic slice cultures. PER2::LUC expression was first measured using a LumiCycle luminometer for 3-4 days to determine whether cultured slices show significant rhythms before transferring them to the

microscope for single-cell analysis. (A) Brightfield (top) and bioluminescence (bottom) images of representative rhythmic (left), arrhythmic (middle), and arrhythmic NAc organotypic slices that were not treated with forskolin (right) (A). (B) Total brightness of arrhythmic NAc slices is lower than of rhythmic NAc slices. (C) Period of single cells in rhythmic and arrhythmic NAc slices is similar, but period of single cells in non-treated arrhythmic NAc slices is significantly shorter than in rhythmic slices. Amplitude of single cells increases after forskolin treatment. This effect is more pronounced in cells from rhythmic NAc explants. Data are shown as mean ± SEM; *p ≤ 0.05 (Student's t-test); cells from rhythmic slices: n = 57, cells from arrhythmic slices: n = 27, cells from arrhythmic, non-treated slices: n = 27. (D) Phase distribution of rhythmic cells is broader in NAc slices whose total PER2::LUC output is arrhythmic than in slices with a rhythmic PER2::LUC output. Data are shown as Rayleigh Plots with the circles representing 24 h of one day and each triangle representing the PER2::LUC phase of an individual cell. The vectors represent the average peak time, and the 95% confidence intervals are shown as an error bar outside of the circle; (Rayleigh's uniformity test) (E) Compared to rhythmic NAc slices, period distribution is broader in NAc slices with an arrhythmic PER2::LUC output. Data are shown as relative frequencies of circadian periods with a non-linear Gaussian regression. The R^2 value describes the goodness of fit of the regression line.

Fig. 7: Single-cell characterization of rhythmic and arrhythmic PAG organotypic slice cultures. (A) Total brightness of rhythmic and arrhythmic PAG slices is similar. (B) Period of single cells in rhythmic and arrhythmic PAG slices is similar. Data are shown as mean ± SEM; cells from rhythmic slices: n = 50, cells from arrhythmic slices: n=36, cells from arrhythmic, non-treated slices: n = 28. (I) Phase distribution of single cells in arrhythmic PAG slices is broader than in

rhythmic slices. Data are shown as in (Fig. 6D); (Rayleigh's uniformity test). (E) Period

distribution of single cells is broader in PAG slices with an arrhythmic PER2::LUC output

compared to slices whose total PER2::LUC output is rhythmic or compared to arrhythmic slices

that were not treated with forskolin. Data are shown as in (Fig. 6E).
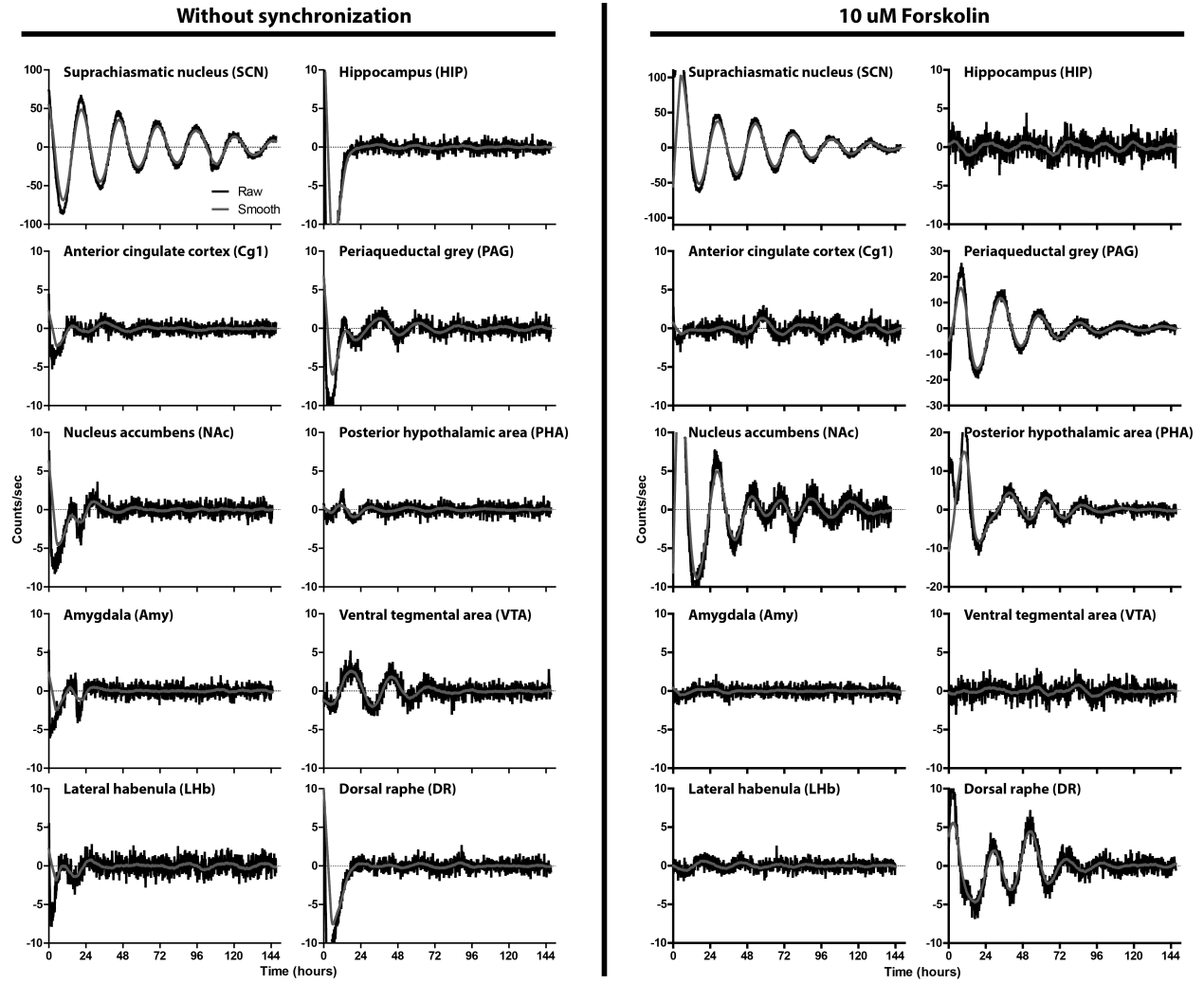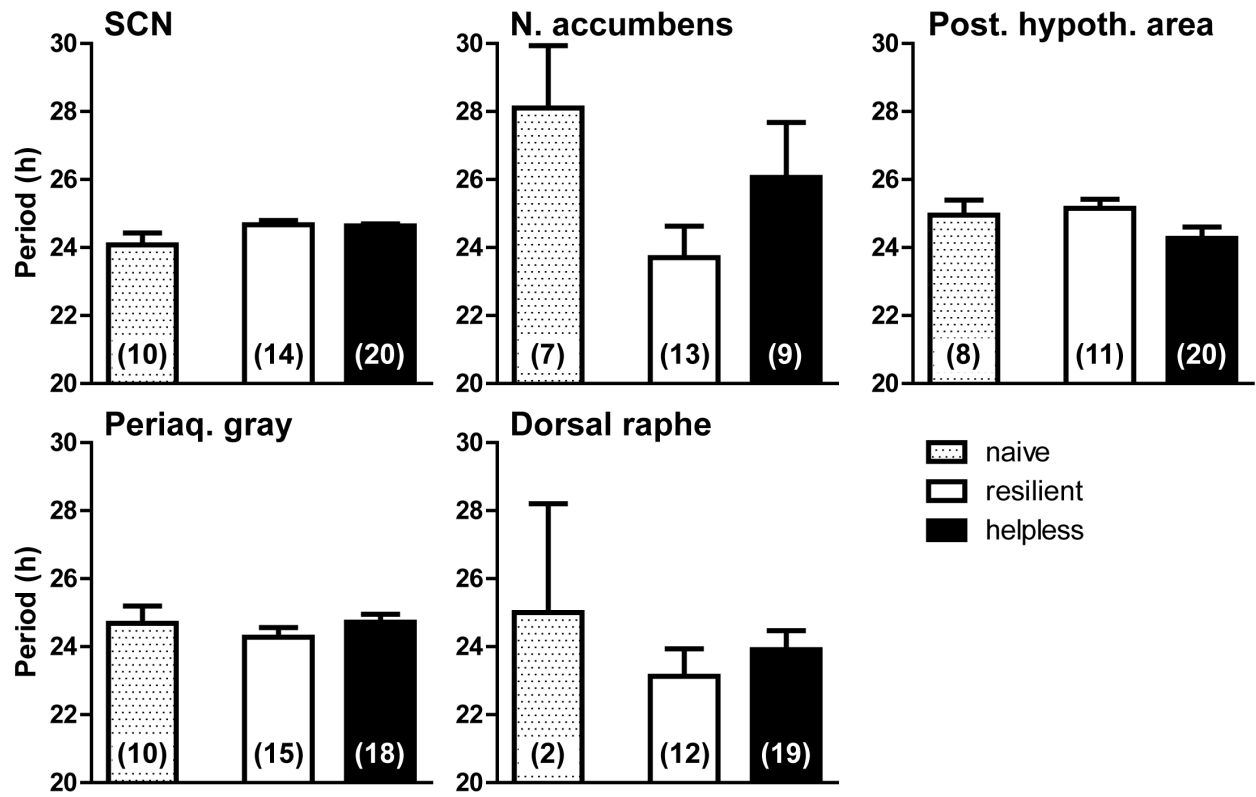
Figures

Figure 1

Figure 2
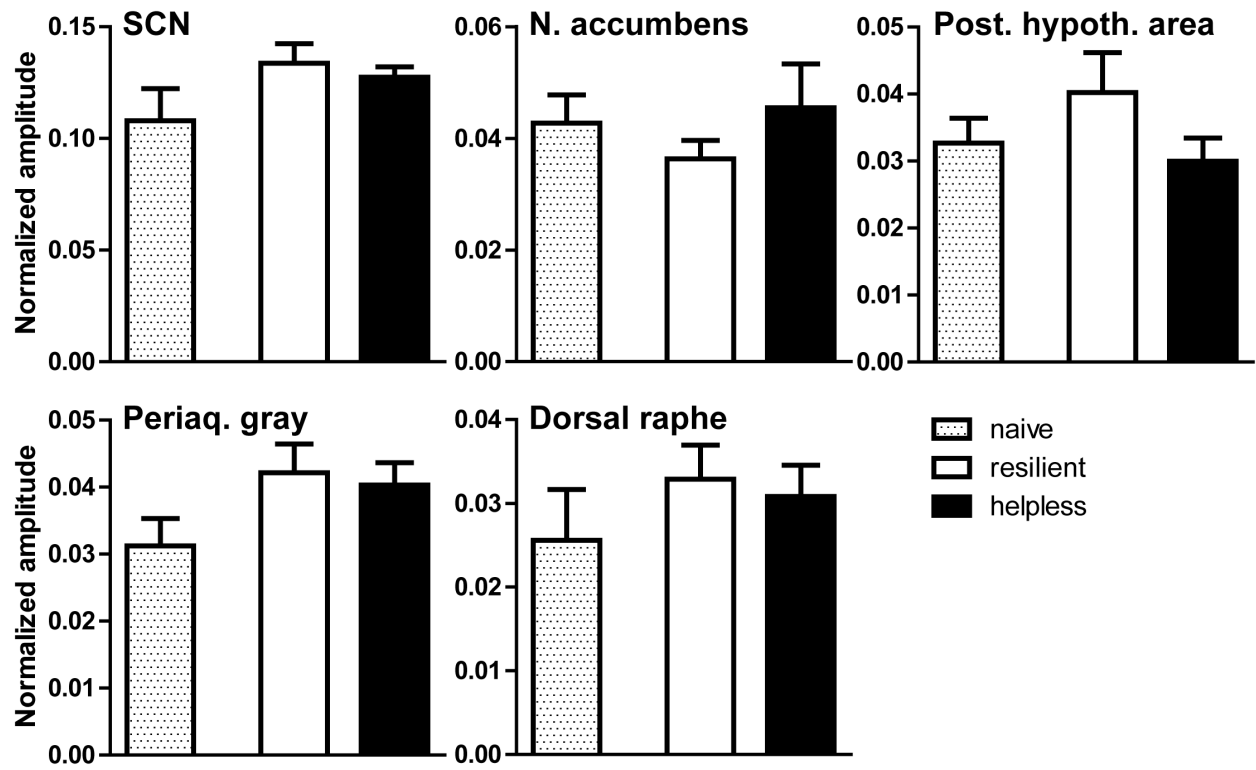
Figure 3

Figure 4

Figure 5

A

Nucleus accumbens

Rhythmic   Arrhythmic   Without forskolin

B Brightness slice

C Period   Amplitude

D

Rhythmic   Arrhythmic   Without forskolin

E

Rhythmic   Arrhythmic   Without forskolin
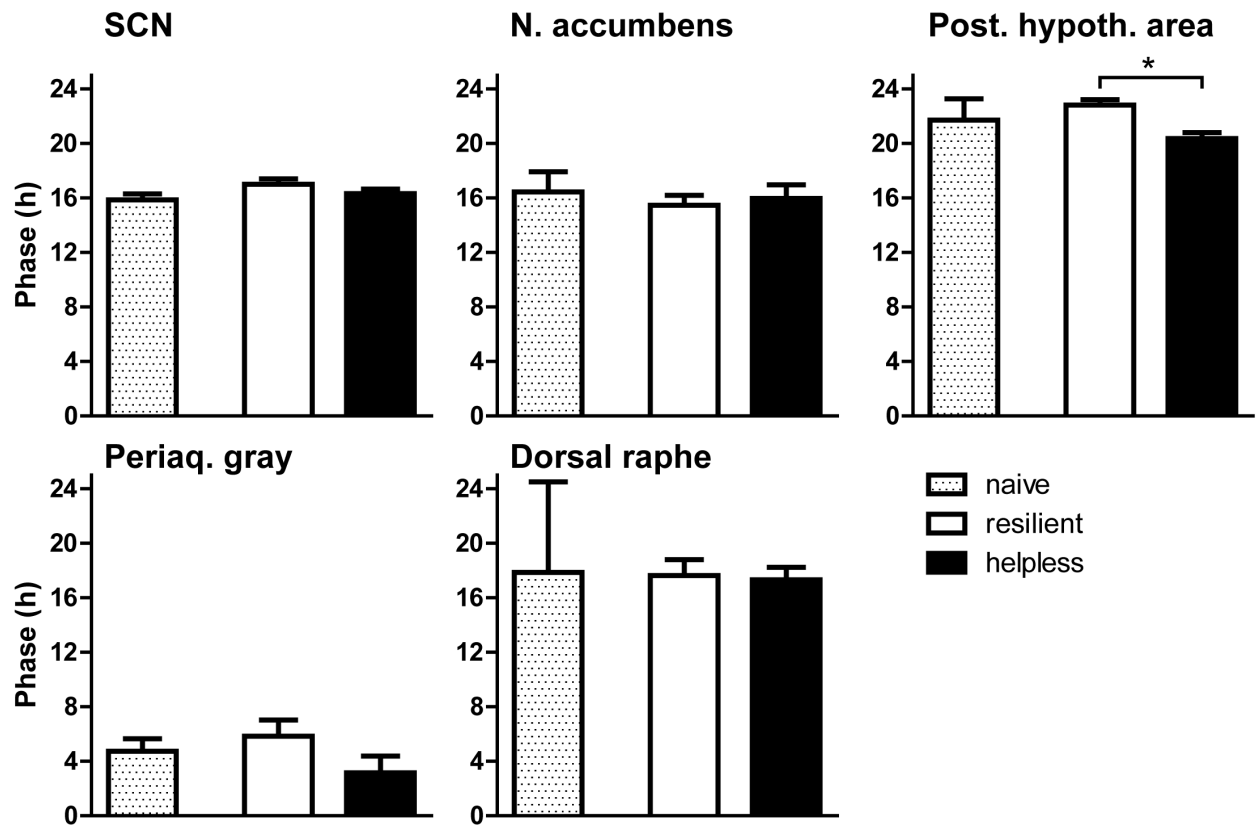
Figure 6

Figure 7

SUPPORTING INFORMATION:

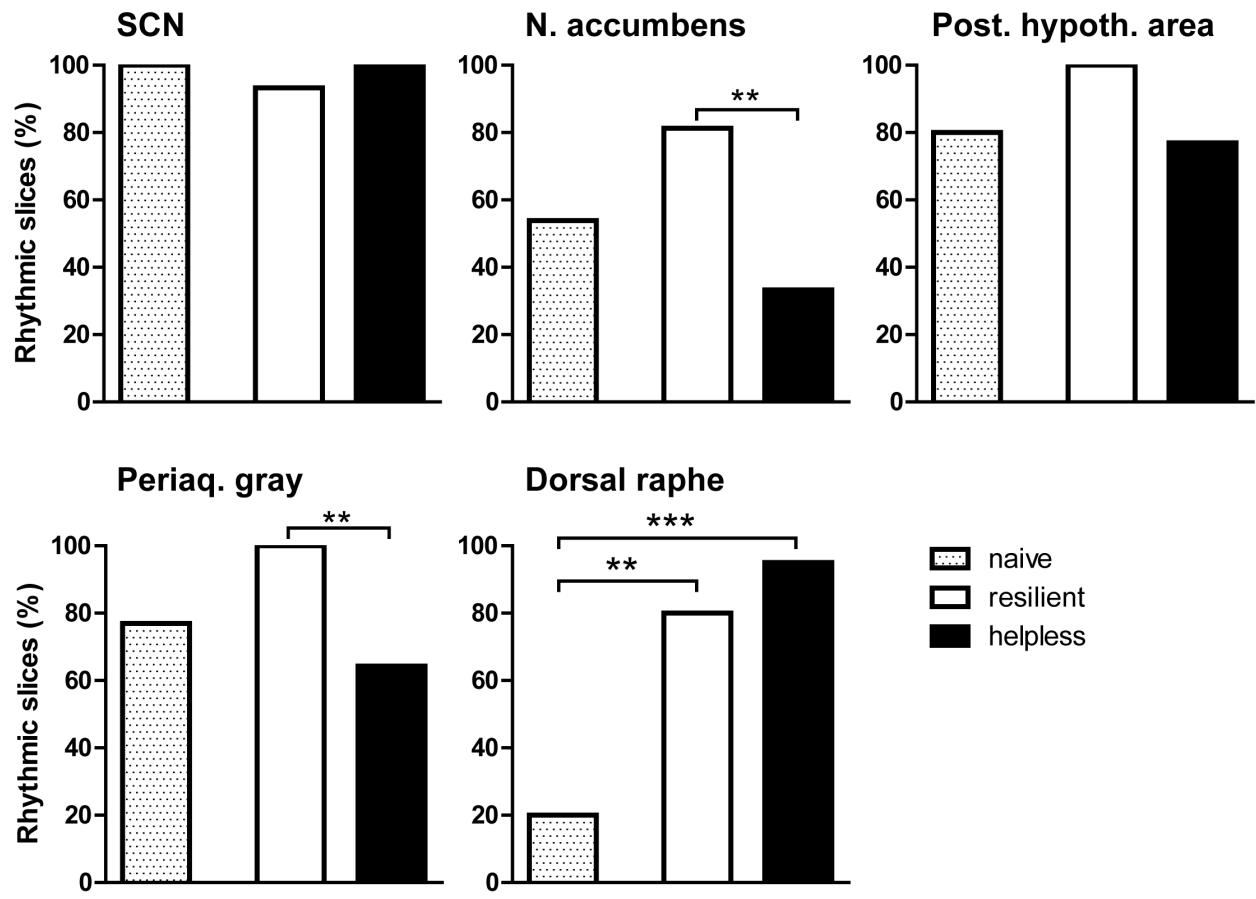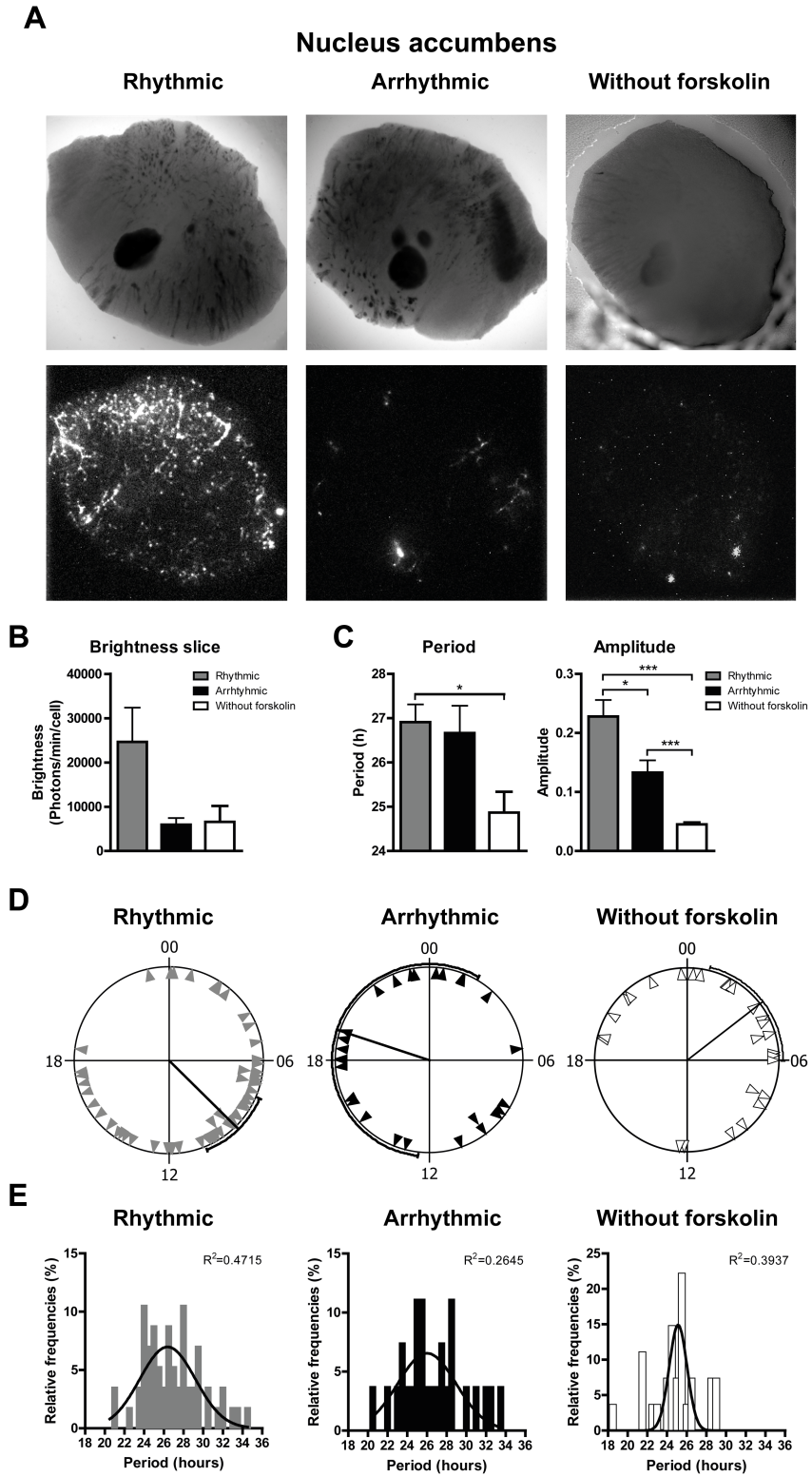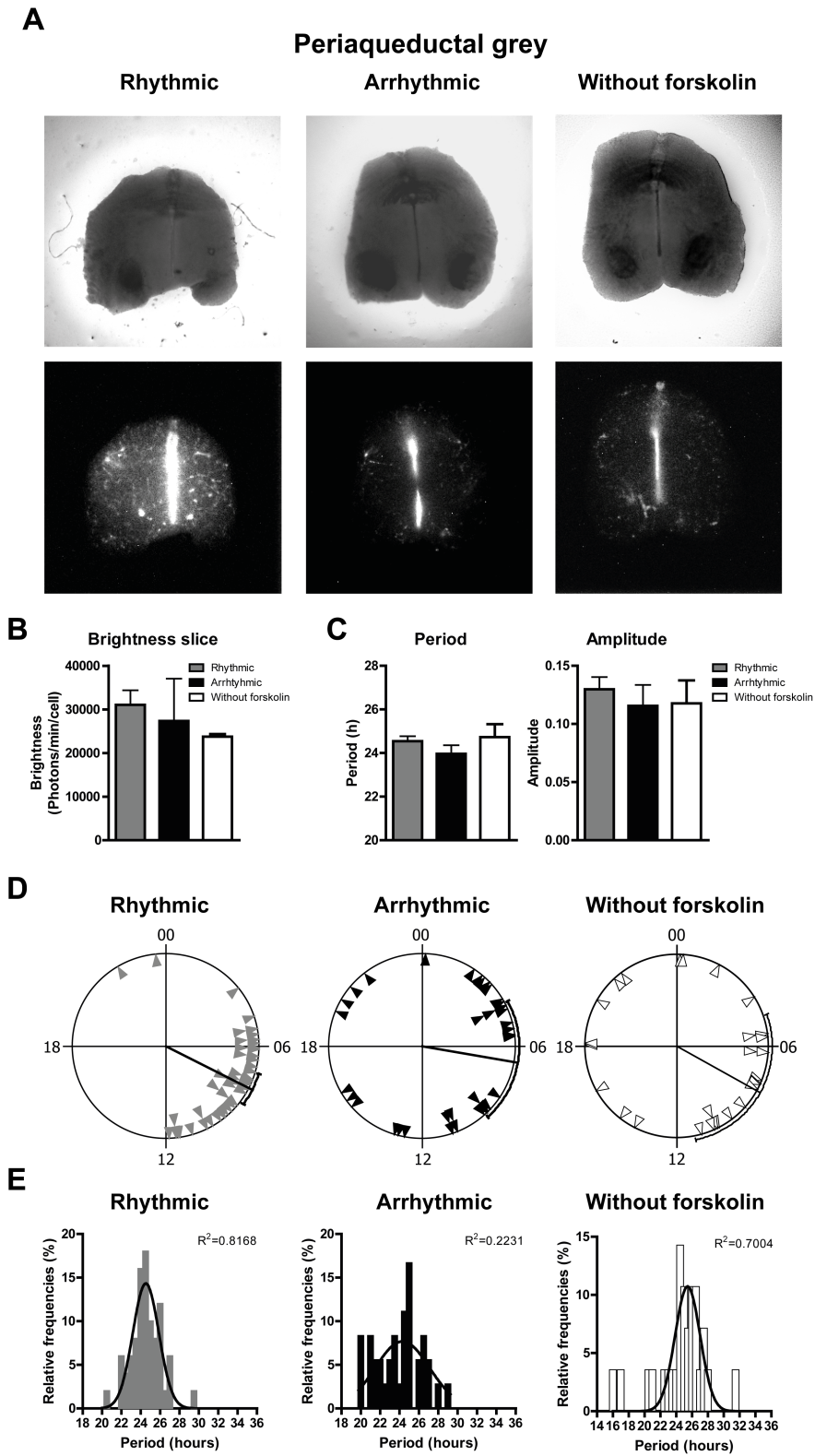**The lateral habenula is less rhythmic than the medial habenula.**

Because of the central role of the LHb in mood regulation (McCarthy & Welsh, 2012), we investigated in more detail the capacity of this brain region to express rhythms. The habenula consists of the LHb and the medial habenula (MHb). It was shown previously that the LHb expresses distinct circadian rhythms whereas the MHb is almost arrhythmic (Guilding *et al.*, 2010). In contrast, our data show opposite results. When measured in the LumiCycle luminometer, rhythms were much stronger in explants containing both MHb and LHb than in explants containing only LHb (Fig. S1A and B). When measured by imaging, we found relatively strong PER2::LUC rhythms in the MHb, but only very faint rhythms in the LHb (Fig. S1C and D).

The LHb receives direct retinal input (Hattar *et al.*, 2006) and is directly innervated by the SCN (Zhang *et al.*, 2009), and it appears to be rhythmic *in vivo* (Zhao & Rusak, 2005; Tavakoli-Nezhad & Schwartz, 2006). However, whether LHb rhythms are endogenously controlled or driven by afferent signals cannot be clarified by *in vivo* studies. The isolated LHb was previously shown to express reliable PER2::LUC rhythms with little contribution from the MHb or rhythmic neuronal activity (Guilding *et al.*, 2010; Sakhi *et al.*, 2014). Since LHb rhythms were rather infrequent in our studies and because of the central role of the LHb in mood regulation, we investigated rhythms of the habenula in more detail. Consistent with previous observations (Guilding *et al.*, 2010), we detected relatively strong rhythms when measuring PER2::LUC signals of the whole habenula, including MHb and LHb. However, when separated from the

MHb, LHb rhythms were absent (Fig. S1). Also, luminescence imaging revealed that in slices

containing both MHb and LHb, MHb exhibited much stronger rhythms than the LHb (Fig. S1),

in contrast to a previous study (Guilding *et al.*, 2010). Our results suggest that although the LHb

is likely rhythmic *in vivo* due to direct retinal and SCN inputs, it has a relatively weak

endogenous clock and is only weakly rhythmic in the absence of any external rhythmic input

signals.

Supplemental figures incl. figure legends:
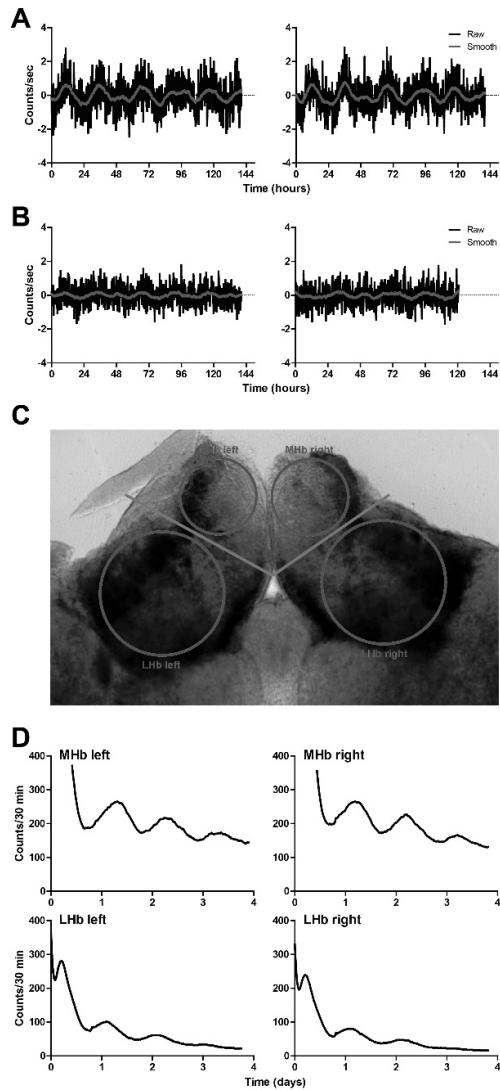
Fig. S1: The lateral habenula shows weaker *in vitro* PER2::LUC rhythms than the medial habenula. (A) Representative rhythms of PER2::LUC expression of the habenula, including lateral and medial habenula, measured in a LumiCycle luminometer. (B) Representative rhythms of PER2::LUC expression of the lateral habenula only, measured in a LumiCycle luminometer. (C) Brightfield image of a cultured habenula. Gray lines mark the border between medial and lateral habenula. Gray circles show the areas of the left and right medial and lateral habenula for which luminescence rhythms were plotted in (D).
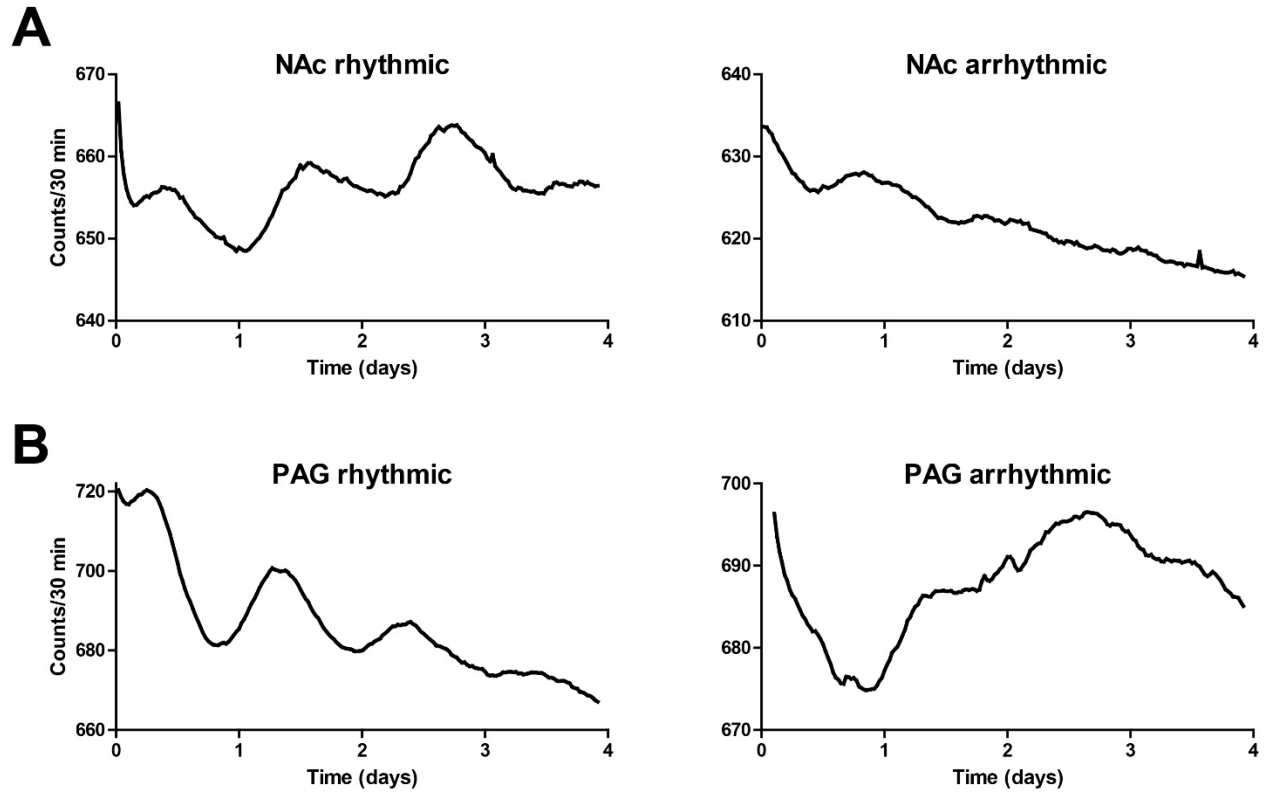
Fig. S2: NAc and PAG explants that appeared arrhythmic in the luminometer show weak or no rhythms when measured by luminescence imaging. (A) Representative PER2::LUC rhythms of a NAc explant that showed significant rhythms in the LumiCycle luminometer (left) and of a NAc explant that failed to show rhythms in the luminometer (right). (B) Representative PER2::LUC rhythms of a PAG explant that showed significant rhythms in the LumiCycle luminometer (left) and of a PAG explant that failed to show rhythms in the luminometer (right).

Table S1: Statistical data from One-way-ANOVA or Welch test comparing PER2::LUC periods obtained from rhythmic brain explants corresponding to Figure 2.

Brain area	Period (h) Mean ± SD			n-value			F-value	p-value	d.f.	Bonferroni post hoc test p-value		
	Naive (A)	Resilient (B)	Helpless (C)	A	B	C				A vs. B	A vs. C	B vs. C
SCN*	24.08 ± 1.10	24.67 ± 0.47	24.64 ± 0.26	10	14	20		0.307	2	n.s.	n.s.	n.s.
NAc	28.10 ± 4.87	23.70 ± 3.34	26.07 ± 4.84	7	13	9	2.593	0.094	2, 26	n.s.	n.s.	n.s.
PHA	24.95 ± 1.25	25.15 ± 0.87	24.27 ± 1.50	8	11	20	1.876	0.168	2, 36	n.s.	n.s.	n.s.
PAG	24.69 ± 1.59	24.28 ± 1.10	24.72 ± 1.02	10	15	18	0.6204	0.543	2, 40	n.s.	n.s.	n.s.
DR	25.00 ± 4.53	23.13 ± 2.77	23.91 ± 2.43	2	12	19	0.6766	0.569	1, 29	--	--	n.s.

* = Welch test due to heterogeneity of variance
d.f. = degrees of freedom
n.s. = not significant
-- = data excluded because n<3
Significant data are bold

Table S2: Statistical data from One-way-ANOVA or Welch test comparing PER2::LUC amplitudes obtained from rhythmic brain explants corresponding to Figure 3.

Brain area	Amplitude (relative unit) Mean ± SD			n-value			F-value	p-value	d.f.	Bonferroni post hoc test p-value		
	Naive (A)	Resilient (B)	Helpless (C)	A	B	C				A vs. B	A vs. C	B vs. C
SCN*	0.1079 ± 0.0454	0.1337 ± 0.0325	0.1274 ± 0.0201	10	14	20		0.342	2	n.s.	n.s.	n.s.
NAc	0.0427 ± 0.0134	0.0363 ± 0.0119	0.0455 ± 0.0236	7	13	9	0.8714	0.430	2, 26	n.s.	n.s.	n.s.
PHA	0.0327 ± 0.0105	0.0402 ± 0.0197	0.0300 ± 0.0154	8	11	20	1.469	0.244	2, 36	n.s.	n.s.	n.s.
PAG	0.0312 ± 0.0130	0.0421 ± 0.0166	0.0403 ± 0.0141	10	15	18	1.787	0.181	2, 40	n.s.	n.s.	n.s.
DR	0.0256 ± 0.0086	0.0329 ± 0.0140	0.0308 ± 0.0162	2	12	19	0.1318	0.808	1, 29	--	--	n.s.

* = Welch test due to heterogeneity of variance
d.f. = degrees of freedom
n.s. = not significant
-- = data excluded because n<3
Significant data are bold

Table S3: Statistical data from One-way-ANOVA or Welch test comparing PER2::LUC phases obtained from rhythmic brain explants corresponding to Figure 4.

Brain area	Phase (hours) Mean ± SD			n-value			F-value	p-value	d.f.	Bonferroni post hoc test p-value		
	Naive (A)	Resilient (B)	Helpless (C)	A	B	C				A vs. B	A vs. C	B vs. C
SCN	15.86 ± 1.40	17.01 ± 1.45	16.33 ± 1.41	10	14	20	2.042	0.143	2, 41	n.s.	n.s.	n.s.
NAc	16.45 ± 3.91	15.46 ± 2.62	15.98 ± 2.98	7	13	9	0.2464	0.783	2, 26	n.s.	n.s.	n.s.
PHA*	21.72 ± 4.39	22.83 ± 1.32	20.36 ± 1.99	8	11	20		**0.04**	2	n.s.	n.s.	**<0.05**
PAG	4.75 ± 2.84	5.84 ± 4.66	3.15 ± 5.21	10	15	18	1.435	0.25	2, 40	n.s.	n.s.	n.s.
DR	17.86 ± 9.41	17.64 ± 4.06	17.32 ± 3.97	2	12	19	0.047	0.971	1, 29	--	--	n.s.

* = Welch test due to heterogeneity of variance
d.f. = degrees of freedom
n.s. = not significant
-- = data excluded because n<3
Significant data are bold

Table S4: Statistical data from Fisher's exact test comparing number of rhythmic and arrhythmic brain area explants corresponding to Figure 5.

Brain area	Rhythmicity (%)			n-value			p-value		
	Naive (A)	Resilient (B)	Helpless (C)	A	B	C	A vs. B	A vs. C	B vs. C
SCN	100.00	93.30	100.00	10	15	20	n.s.	n.s.	n.s.
NAc	53.85	81.25	33.33	13	16	27	n.s.	n.s.	**< 0.01**
PHA	80.00	100.00	76.92	10	11	26	n.s.	n.s.	n.s.
PAG	76.92	100.00	64.29	13	15	28	n.s.	n.s.	**< 0.01**
DR	20.00	80.00	95.00	10	15	20	**< 0.01**	**< 0.001**	n.s.

d.f. = degrees of freedom
n.s. = not significant
Significant data are bold

Table S5: : Statistical data from One-way-ANOVA or Kruskal-Wallis test comparing PER2::LUC periods and amplitudes obtained from single cells of rhythmic and arrhythmic NAc explants corresponding to Figure 6. Post-hoc test for One-way-ANOVA: Bonferroni. Post-hoc test for Kruskal-Wallis test: Dunn's Multiple Comparison test.

Parameter	Group			n-value			F-value	p-value	d.f.	Post-hoc test p-value		
	Rhythmic (A)	Arrhythmic (B)	w/o Forsk. (C)	A	B	C				A vs. B	A vs. C	B vs. C
Brightness slice (Photons/min/cell)	24635 ± 10936	5953 ± 2097	6594 ± 5075	2	2	2	--	--	--	--	--	--
Period (h)	26.91 ± 3.02	26.67 ± 3.19	24.87 ± 2.442	57	27	27	4.650	**0.012**	2, 108	n.s.	**0.011**	n.s.
Amplitude (rel. unit)[#]	0.2297 ± 0.2115	0.1330 ± 0.1074	0.0452 ± 0.0168	57	27	27		**< 0.001**		**< 0.05**	**< 0.001**	**< 0.001**

-- = data excluded because n<3
d.f. = degree of freedom
[#] = Kruskal-Wallis test due to non-normal distributed data
Significant data are bold

Table S6: Statistical data from Rayleigh's uniformity test analyzing phase distribution from single cells of rhythmic and arrhythmic NAc explants corresponding to Figure 6.

Parameter	Group			n-value			p-value		
	Rhythmic	Arrhythmic	w/o Forsk.	Rhythmic	Arrhythmic	w/o Forsk.	Rhythmic	Arrhythmic	w/o Forsk.
Data distribution (Z-value)	11.497	0.602	3.994	57	27	27	**1.02E-5**	0.552	**0.017**

Significant data are bold

Table S7: Statistical data from Welch test or Kruskal-Wallis test comparing PER2::LUC periods and amplitudes obtained from single cells of rhythmic and arrhythmic PAG explants corresponding to Figure 6. Post-hoc test for Welsh test: Bonferroni. Post-hoc test for Kruskal-Wallis test: Dunn's Multiple Comparison test.

Parameter	Group			n-value			d.f.	p-value	Post-hoc test p-value		
	Rhythmic (A)	Arrhythmic (B)	w/o Forsk. (C)	A	B	C			A vs. B	A vs. C	B vs. C
Brightness slice (Photons/min/cell)	31048 ± 4709	27362 ± 13679	23759 ± 847	2	2	2	--	--	--	--	--
Period (h)*	24.54 ± 1.06	23.96 ± 2.36	24.73 ± 3.15	50	36	28	2	0.392	n.s.	n.s.	n.s.
Amplitude (rel. unit)#	0.1298 ± 0.0742	0.1156 ± 0.1077	0.1177 ± 0.1046	50	36	28		0.090	n.s.	n.s.	n.s.

* = Welch test due to heterogeneity of variance
# = Kruskal-Wallis test due to non-normal distributed data
-- = data excluded because n<3
d.f. = degree of freedom

Table S8: Statistical data from Rayleigh's uniformity test analyzing phase distribution from single cells of rhythmic and arrhythmic PAG explants corresponding to Figure 6.

Parameter	Group			n-value			p-value		
	Rhythmic	Arrhythmic	w/o Forsk.	Rhythmic	Arrhythmic	w/o Forsk.	Rhythmic	Arrhythmic	w/o Forsk.
Data distribution (Z-value)	32.778	4.145	2.492	50	36	28	**< 1E-12**	**0.015**	0.082

Significant data are bold

References Supporting information:

Balsalobre, A., Brown, S.A., Marcacci, L., Tronche, F., Kellendonk, C., Reichardt, H.M., Schutz, G. & Schibler, U. (2000) Resetting of circadian time in peripheral tissues by glucocorticoid signaling. *Science*, **289**, 2344-2347.

Berton, O., Covington, H.E., 3rd, Ebner, K., Tsankova, N.M., Carle, T.L., Ulery, P., Bhonsle, A., Barrot, M., Krishnan, V., Singewald, G.M., Singewald, N., Birnbaum, S., Neve, R.L. & Nestler, E.J. (2007) Induction of deltaFosB in the periaqueductal gray by stress promotes active coping responses. *Neuron*, **55**, 289-300.

Boyce, P. & Barriball, E. (2010) Circadian rhythms and depression. *Australian family physician*, **39**, 307-310.

Buhr, E.D., Yoo, S.H. & Takahashi, J.S. (2010) Temperature as a universal resetting cue for mammalian circadian oscillators. *Science*, **330**, 379-385.

Eskin, A. & Takahashi, J.S. (1983) Adenylate cyclase activation shifts the phase of a circadian pacemaker. *Science*, **220**, 82-84.

Grahn, R.E., Will, M.J., Hammack, S.E., Maswood, S., McQueen, M.B., Watkins, L.R. & Maier, S.F. (1999) Activation of serotonin-immunoreactive cells in the dorsal raphe nucleus in rats exposed to an uncontrollable stressor. *Brain research*, **826**, 35-43.

Guilding, C., Hughes, A.T. & Piggins, H.D. (2010) Circadian oscillators in the epithalamus. *Neuroscience*, **169**, 1630-1639.

Hattar, S., Kumar, M., Park, A., Tong, P., Tung, J., Yau, K.W. & Berson, D.M. (2006) Central projections of melanopsin-expressing retinal ganglion cells in the mouse. *The Journal of comparative neurology*, **497**, 326-349.

Herpfer, I. & Lieb, K. (2005) Substance P receptor antagonists in psychiatry: rationale for development and therapeutic potential. *CNS drugs*, **19**, 275-293.

Jiang, W.G., Li, S.X., Zhou, S.J., Sun, Y., Shi, J. & Lu, L. (2011) Chronic unpredictable stress induces a reversible change of PER2 rhythm in the suprachiasmatic nucleus. *Brain research*, **1399**, 25-32.

Kelleher, F.C., Rao, A. & Maguire, A. (2014) Circadian molecular clocks and cancer. *Cancer letters*, **342**, 9-18.

Landgraf, D., Long, J., Der-Avakian, A., Streets, M. & Welsh, D.K. (2015) Dissociation of learned helplessness and fear conditioning in mice: a mouse model of depression. *PloS one*, **10**, e0125892.

Landgraf, D., McCarthy, M.J. & Welsh, D.K. (2014a) Circadian clock and stress interactions in the molecular biology of psychiatric disorders. *Current psychiatry reports*, **16**, 483.

Landgraf, D., McCarthy, M.J. & Welsh, D.K. (2014b) The role of the circadian clock in animal models of mood disorders. *Behavioral neuroscience*, **128**, 344-359.

Li, J.Z., Bunney, B.G., Meng, F., Hagenauer, M.H., Walsh, D.M., Vawter, M.P., Evans, S.J., Choudary, P.V., Cartagena, P., Barchas, J.D., Schatzberg, A.F., Jones, E.G., Myers, R.M., Watson, S.J., Jr., Akil, H. & Bunney, W.E. (2013) Circadian patterns of gene expression in the human brain and disruption in major depressive disorder. *Proceedings of the National Academy of Sciences of the United States of America*, **110**, 9950-9955.

Liu, A.C., Welsh, D.K., Ko, C.H., Tran, H.G., Zhang, E.E., Priest, A.A., Buhr, E.D., Singer, O., Meeker, K., Verma, I.M., Doyle, F.J., 3rd, Takahashi, J.S. & Kay, S.A. (2007) Intercellular coupling confers robustness against mutations in the SCN circadian clock network. *Cell*, **129**, 605-616.

Logan, R.W., Edgar, N., Gillman, A.G., Hoffman, D., Zhu, X. & McClung, C.A. (2015) Chronic Stress Induces Brain Region-Specific Alterations of Molecular Rhythms that Correlate with Depression-like Behavior in Mice. *Biological psychiatry*.

Maier, S.F., Grahn, R.E., Kalman, B.A., Sutton, L.C., Wiertelak, E.P. & Watkins, L.R. (1993) The role of the amygdala and dorsal raphe nucleus in mediating the behavioral consequences of inescapable shock. *Behavioral neuroscience*, **107**, 377-388.

Maier, S.F., Grahn, R.E. & Watkins, L.R. (1995) 8-OH-DPAT microinjected in the region of the dorsal raphe nucleus blocks and reverses the enhancement of fear conditioning and interference with escape produced by exposure to inescapable shock. *Behavioral neuroscience*, **109**, 404-412.

Maier, S.F. & Watkins, L.R. (2005) Stressor controllability and learned helplessness: the roles of the dorsal raphe nucleus, serotonin, and corticotropin-releasing factor. *Neuroscience and biobehavioral reviews*, **29**, 829-841.

McCarthy, M.J. & Welsh, D.K. (2012) Cellular circadian clocks in mood disorders. *Journal of biological rhythms*, **27**, 339-352.

Morris, C.J., Yang, J.N. & Scheer, F.A. (2012) The impact of the circadian timing system on cardiovascular and metabolic function. *Progress in brain research*, **199**, 337-358.

Noguchi, T., Wang, L.L. & Welsh, D.K. (2013) Fibroblast PER2 circadian rhythmicity depends on cell density. *Journal of biological rhythms*, **28**, 183-192.

Russo, S.J. & Nestler, E.J. (2013) The brain reward circuitry in mood disorders. *Nature reviews. Neuroscience*, **14**, 609-625.

Sakhi, K., Wegner, S., Belle, M.D., Howarth, M., Delagrange, P., Brown, T.M. & Piggins, H.D. (2014) Intrinsic and extrinsic cues regulate the daily profile of mouse lateral habenula neuronal activity. *The Journal of physiology*.

Sancar, G. & Brunner, M. (2014) Circadian clocks and energy metabolism. *Cellular and molecular life sciences : CMLS*, **71**, 2667-2680.

Savalli, G., Diao, W., Schulz, S., Todtova, K. & Pollak, D.D. (2015) Diurnal oscillation of amygdala clock gene expression and loss of synchrony in a mouse model of depression. *Int J Neuropsychopharmacol*, **18**.

Schutz, M.T., de Aguiar, J.C. & Graeff, F.G. (1985) Anti-aversive role of serotonin in the dorsal periaqueductal grey matter. *Psychopharmacology*, **85**, 340-345.

Sokolove, P.G. & Bushell, W.N. (1978) The chi square periodogram: its utility for analysis of circadian rhythms. *Journal of theoretical biology*, **72**, 131-160.

Spencer, S., Falcon, E., Kumar, J., Krishnan, V., Mukherjee, S., Birnbaum, S.G. & McClung, C.A. (2013) Circadian genes Period 1 and Period 2 in the nucleus accumbens regulate anxiety-related behavior. *The European journal of neuroscience*, **37**, 242-250.

Tavakoli-Nezhad, M. & Schwartz, W.J. (2006) Hamsters running on time: is the lateral habenula a part of the clock? *Chronobiology international*, **23**, 217-224.

Welsh, D.K. & Noguchi, T. (2012) Cellular bioluminescence imaging. *Cold Spring Harbor protocols*, **2012**.

Welsh, D.K., Yoo, S.H., Liu, A.C., Takahashi, J.S. & Kay, S.A. (2004) Bioluminescence imaging of individual fibroblasts reveals persistent, independently phased circadian rhythms of clock gene expression. *Current biology : CB*, **14**, 2289-2295.

Yagita, K. & Okamura, H. (2000) Forskolin induces circadian gene expression of rPer1, rPer2 and dbp in mammalian rat-1 fibroblasts. *FEBS letters*, **465**, 79-82.

Yoo, S.H., Yamazaki, S., Lowrey, P.L., Shimomura, K., Ko, C.H., Buhr, E.D., Siepka, S.M., Hong, H.K., Oh, W.J., Yoo, O.J., Menaker, M. & Takahashi, J.S. (2004) PERIOD2::LUCIFERASE real-time reporting of circadian dynamics reveals persistent circadian oscillations in mouse peripheral tissues. *Proceedings of the National Academy of Sciences of the United States of America*, **101**, 5339-5346.

Zhang, C., Truong, K.K. & Zhou, Q.Y. (2009) Efferent projections of prokineticin 2 expressing neurons in the mouse suprachiasmatic nucleus. *PloS one*, **4**, e7151.

Zhao, H. & Rusak, B. (2005) Circadian firing-rate rhythms and light responses of rat habenular nucleus neurons in vivo and in vitro. *Neuroscience*, **132**, 519-528.